AD-A147 480 ELECTROSTATIC WAVE OBSERVATION DURING A SPACE SIMULATION BEAM-PLASMA-DISCHARGE(U) NAVAL RESEARCH LAB WASHINGTON DC D N WALKER ET AL. 19 NOV 84 NRL-MR-5434 1/1

UNCLASSIFIED F/G 20/9 NL

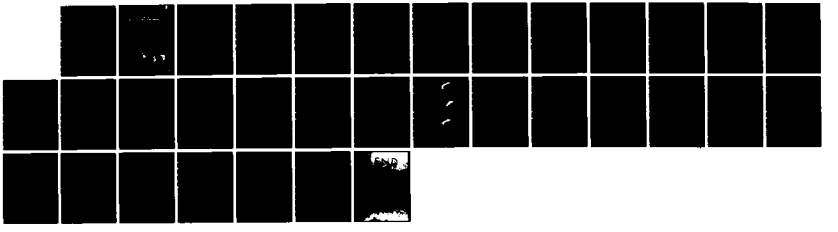

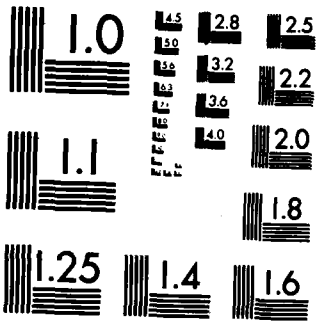
1.0
1.1
1.25
1.4
1.6
1.8
2.0
2.2
2.5
2.8
3.2
3.6
4.0
4.5
5.0
5.6
6.3

NRL Memorandum Report 5434

Electrostatic Wave Observation During a Space Simulation Beam-Plasma-Discharge

D. N. WALKER AND E. P. SZUSZCZEWICZ

Space Plasma Physics and Applications Research Group
Plasma Physics Division

November 19, 1984

This work was supported by the Office of Naval Research.

NAVAL RESEARCH LABORATORY
Washington, D.C.

SECURITY CLASSIFICATION OF THIS PAGE

REPORT DOCUMENTATION PAGE

1a REPORT SECURITY CLASSIFICATION UNCLASSIFIED	1b RESTRICTIVE MARKINGS
2a SECURITY CLASSIFICATION AUTHORITY	3 DISTRIBUTION/AVAILABILITY OF REPORT Approved for public release; distribution unlimited.
2b DECLASSIFICATION/DOWNGRADING SCHEDULE	
4 PERFORMING ORGANIZATION REPORT NUMBER(S) NRL Memorandum Report 5434	5 MONITORING ORGANIZATION REPORT NUMBER(S)
6a NAME OF PERFORMING ORGANIZATION Naval Research Laboratory 6b OFFICE SYMBOL (If applicable) Code 4108	7a NAME OF MONITORING ORGANIZATION
6c ADDRESS (City, State, and ZIP Code) Washington, DC 20375-5000	7b ADDRESS (City, State, and ZIP Code)
8a NAME OF FUNDING/SPONSORING ORGANIZATION Office of Naval Research 8b OFFICE SYMBOL (If applicable)	9 PROCUREMENT INSTRUMENT IDENTIFICATION NUMBER
8c ADDRESS (City, State, and ZIP Code) Arlington, VA 22217	10 SOURCE OF FUNDING NUMBERS PROGRAM ELEMENT NO: 61153N; PROJECT NO:; TASK NO: RR033-02-44; WORK UNIT ACCESSION NO: DN620-160

11 TITLE (Include Security Classification)

Electrostatic Wave Observation During a Space Simulation Beam-Plasma-Discharge

12 PERSONAL AUTHOR(S)
Walker, D.N. and Szuszczewicz, E.P.

13a TYPE OF REPORT	13b TIME COVERED	14 DATE OF REPORT (Year, Month, Day)	15 PAGE COUNT
Interim	FROM _____ TO _____	1984 November 19	33

16 SUPPLEMENTARY NOTATION

This work was supported by the Office of Naval Research.

17 COSATI CODES			18 SUBJECT TERMS (Continue on reverse if necessary and identify by block number)		
FIELD	GROUP	SUB-GROUP	Waves	Space simulation	Cross-correlation
			Plasma physics	Langmuir probes	

19 ABSTRACT (Continue on reverse if necessary and identify by block number)

In continuing the investigation of a series of space simulation experiments in the large vacuum chamber at the Johnson Space Center, we have analyzed observed ELF waves through associated measurements of electron density, electron temperature, plasma potential, power spectral density, and cross-correlation spectra. The experimental condition was that of a Beam-Plasma-Discharge (BPD) with an electron gun voltage of 1.6 keV and a beam current of 40 ma in an external magnetic field of 1.5 gauss. Phase delays (obtained from cross-correlation measurements of density fluctuations) along with the measurements of plasma potential and frequency as a function of radius have been used to compare our results to a zero-order slab model of non-local azimuthal drift wave propagation. Based on the results of plasma potential measurements, the laboratory rotational velocities obtained from frequency observations have been corrected for $E \times B$ Doppler shift to compare with theory in the plasma frame. In particular the inferred wave phase velocity in the plasma frame

(Continues)

20 DISTRIBUTION/AVAILABILITY OF ABSTRACT	21 ABSTRACT SECURITY CLASSIFICATION
☒ UNCLASSIFIED/UNLIMITED ☐ SAME AS RPT ☐ DTIC USERS	UNCLASSIFIED
22a NAME OF RESPONSIBLE INDIVIDUAL D. N. Walker	22b TELEPHONE (Include Area Code) (202) 767-2248 22c OFFICE SYMBOL Code 4108

DD FORM 1473, 84 MAR 83 APR edition may be used until exhausted
All other editions are obsolete

SECURITY CLASSIFICATION OF THIS PAGE

19. **ABSTRACT** (Continued) the authors' her

is found to be near one-half the electron diamagnetic drift velocity based on observations and the equilibrium drift correction. Although our measurements do not uniquely define a propagation mode, we discuss a model of azimuthal drift wave propagation which is consistent with our observations.

CONTENTS

I. INTRODUCTION 1

II. EXPERIMENTAL CONFIGURATION 2

III. EXPERIMENTAL TECHNIQUE AND RESULTS 3

IV. DISCUSSION AND INTERPRETATION OF RESULTS 5

V. CONCLUSIONS 14

VI. ACKNOWLEDGMENT 14

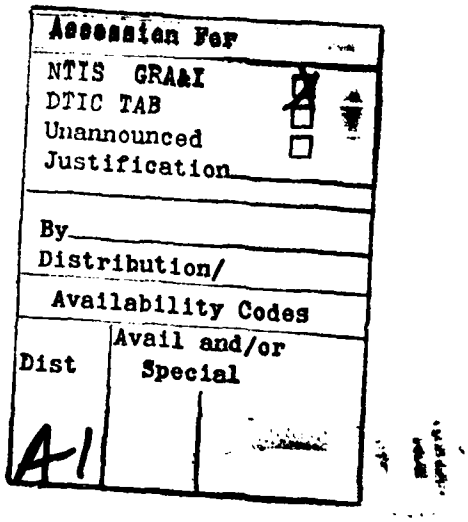

ELECTROSTATIC WAVE OBSERVATION DURING A SPACE SIMULATION BEAM-PLASMA-DISCHARGE

I. INTRODUCTION

The Beam-Plasma-Discharge (BPD) instability (Getty and Smullin, 1963) has re-emerged in recent years (Smullin, 1981; Bernstein et al., 1978) as a fundamental process to be considered by designers of space vehicle-borne electron accelerator experiments. Because of concerns over vehicle neutralization during these experiments and an interest in further understanding of the BPD process (Cambou, 1975, 1978) a series of space simulation investigations of the BPD phenomenon was undertaken in the large vacuum chamber facility at Johnson Space Center (Bernstein 1978, 1979; Szuszczewicz 1979, 1982a; Papadopoulos, 1982; Anderson, 1981). Bernstein, et al. 1979 were able to conclude that the phenomenon is dependent upon a critical electron beam current, I_B^c, for ignition and that

$$I_B^c \propto V_B^{3/2} \; B^{-.7} \; P^{-1} L^{-1} \qquad (1)$$

where V_B is the beam energy in volts, B the magnetic field in gauss, P the ambient neutral particle pressure in torr, and L the beam length in meters.

The BPD is characterized by a transition from single particle to collective processes. Further characteristics of BPD include enhanced electron densities and spatial broadening of the beam. In addition, there are a number of plasma mode oscillations excited which extend from plasma waves at frequencies near the local plasma frequency down to electron cyclotron and extremely low frequency (ELF) electrostatic oscillations. In a previous paper (Szuszczewicz et al., 1982a) we established a density dependent criterion for BPD ignition. In the present paper we examine ELF density oscillations along with plasma potential and frequency measurements and discuss a model of azimuthal wave propagation which is consistent with our observations.

Manuscript approved June 21, 1984.

Low frequency drift wave instabilities have long been associated with energy transport and anomalous diffusion in turbulent plasma regimes and have hence been an important topic in studies of plasma confinement (Kadomtsev, 1965). In low-β space applications the sharp density gradients encountered in the equatorial ionospheric studies of spread-F (Ossakow, 1981; Huba and Ossakow, 1979; Singh and Szuszczewicz, 1984; Kelley, 1982; Gary, 1983; Szuszczewicz, et al., 1982b) are often sufficient to produce low frequency drift instabilities. In the laboratory environment described here, earlier investigations of the BPD phenomenon (Szuszczewicz, et al., 1979) yielded estimates of perpendicular diffusion coefficients orders of magnitude higher than predicted for classical collisional diffusion. Those results were consistent with a Bohm-like diffusion process created by wave turbulence. The current experimental configuration, described below, is an outgrowth of these results and a recognition of the desirability of further quantifying the wave measurements.

II. EXPERIMENTAL CONFIGURATION

The experiment was conducted in the large vacuum chamber at the Johnson Space Center with a configuration similar to earlier investigations of Bernstein et al., 1979. The primary diagnostic was the pulsed-plasma-probe, P^3, system illustrated in Figures 1A and 1B. Figure 1A is a schematic view of the cylindrical chamber showing the position of the electron gun and collector plate. The magnetic field maintained during the BPD investigation was held constant at 1.5 gauss and was a result of the ambient field and the field produced by the Helmholtz coils pictured in the Figure. Figure 1B is a top view of the chamber showing the traversal axis of the P^3 system with respect to the gun-collector position within the chamber. A complete probe system traversal consisted of a cycle from A to B and back.

The beam was generated by a tungsten-cathode Pierce-type diode gun and was aligned as closely as possible to the magnetic field.

The plasma was generated by beam injection into the ambient neutral gas (i.e., air) at pressures near 10^{-6} torr. For the case studied here the beam energy was 1.6 kev and beam current was 40 ma. A relative electron density profile for a complete traversal during BPD is shown as the upper plot in Figure 2. The abscissa is time measured from the beginning of a traversal and the vertical lines drawn in the figure identify a point approximately 0.6m radially outward from the beam center and effectively demarcate the beam core boundary during BPD. In addition shown in Figures 2A-2C are radial profiles of electron density, electron temperature and plasma potential. An exponential least squares best fit to each data set is also shown in these Figures. The abscissa is radial distance with respect to the beam center.

III. EXPERIMENTAL TECHNIQUE AND RESULTS

The experimental configuration of a two-probe system in which the probes are one meter apart along the radius provides a 2-point measurement for phase delay calculations using cross-correlation signal analysis techniques (Bendat and Piersol, 1971).

The basic operating mode of the two-probe P^3 system provides a continuous two-point determination of relative density variations through measurement of electron and ion saturation currents in addition to the simultaneous determination of absolute densities, temperatures and plasma potentials through characteristic Langmuir probe response to an applied sweep voltage. This is accomplished through a pulsing procedure which alternately pulses the probe between an applied sweep voltage and a fixed-bias level (electron saturation for the E-Probe and ion saturation for the I-Probe). In this experiment the two-point cross-correlation measurements were done using E- and

I-probe fixed bias levels. Each of these current fluctuations is proportional to density and, in the absence of potential variations or ion mass changes, would be in phase in a homogeneous neutral plasma.

The basis of the cross-correlation technique is the integral,

$$C(\tau) = \lim_{T\to\infty} \frac{1}{T} \int_0^T \left| \frac{\delta I_{BE}(t)}{\overline{I}_{BE}} \right\| \frac{\delta I_{BI}(t+\tau)}{I_{BI}} \Bigg| \, dt \qquad (2)$$

where $I_{BE}(t)$ is electron-saturation current collected by the E-probe (at a fixed positive bias) and $I_{BI}(t)$ is ion-saturation current collected by the I-probe (at fixed negative bias) which is positioned 1 meter radially outward from the E-probe. The currents are detrended using a least squares fit to the data and fluctuations from this fit, $\delta I_{BE(I)}$, were normalized by the fitted value.

Figure 3 is a sample of a .25 second interval of data taken near r_E = 2.5 meters from beam center where r_E indicates the E-probe position relative to beam center. Illustrated in Figure 3 is the time delay τ_o ($\sim$ 10 msec) of the wave train passing through the two-probe system. τ_o is shown more clearly in the plot of $C(\tau)$ in Figure 4, where the integration interval was 1.2 seconds and the sample frequency was 500 Hz. Since a general waveform such as $C(\tau)$ can be composed of a number of prime discrete frequencies, it is necessary to decompose the waveform in order to uniquely associate phase shift with frequency. The Fourier transform of $C(\tau)$, referred to as the cross-spectral density function ($F_c(i\omega)$), accomplishes this decomposition and is generally a complex number,

$$F_C(i\omega) = |F_C(i\omega)| e^{-i(\omega\tau)_{I_{BE},I_{BI}}} \qquad (3)$$

In this form $(\omega\tau)_{I_{BE},I_{BI}}$ is the phase shift of the frequency component ω, and τ is the time delay of propagation through the two-probe system. The cross spectral density in Figure 5 shows a peak near 45 Hz and a phase shift near 2.6 radians consistent with the time delay (τ_o) in Figure 4.

It is appropriate to point out here that for certain non-local propagating drift modes (Chen, 1967) in cylindrical coordinates, radially displaced sensors would detect a phase difference in density oscillations at their separate positions (Hooper, 1970). For example, for an azimuthal density fluctuation of the form $n(r)\, e^{i(m\theta-\omega t)}$ where the radial wave number, k_r, is less than the inverse probe separation (i.e. $k_r<|r_e-r_i|^{-1}$) there is the possibility of a radial dependence to the azimuthal phase shift as shown pictorially in Figure 7 (see for example, Hooper et al, 1983 which is similar to that illustrated here). With our sensor orientation along the radial direction as depicted and with the radial oscillation amplitude of the same order of magnitude as the azimuthal wavelength (Ellis and Motley, 1974; Chen, 1967) there is pictured a monotonically increasing phase shift as a function of radius at the two positions. Of course without the addition of a 3rd probe in the azimuthal direction it is impossible to uniquely associate a propagation direction, $\hat{k}$, with a measured phase delay. However, based on physical arguments below, we feel that identification of our measurements with some form of drift mode propagation is reasonable.

IV. DISCUSSION AND INTERPRETATION OF RESULTS

It is well known that a magnetized plasma with density and/or temperature gradients can support plasma oscillations perpendicular to $\bar{B}$ with phase velocities near the diamagnetic drift velocity (Krall and Trivelpiece, 1973).

For a low-β plasma with gradients in electron density and temperature along $-\hat{x}$ in a magnetic field $\bar{B} = B_o\hat{z}$ (see Figure 6), the pressure balance

requirement in the absence of an equilibrium electric field yields a zero-order electron diamagnetic drift of,

$$\bar{V}_D = + \frac{cKT_e}{eB_0} \left(\frac{1}{n} \frac{\partial n}{\partial x} + \frac{1}{T} \frac{\partial T}{\partial X} \right) \hat{y} \tag{4}$$

Plotted in Figure 2A and 2B are equilibrium electron density and temperature profiles along with exponential fits to the data. From these results and the slab model assumption as shown in Figure 6

$$\bar{\nabla} n = - \left| \frac{\partial n}{\partial x} \right| \hat{x}, \quad \bar{\nabla} T_e = - \left| \frac{\partial T}{\partial x} \right| \hat{x} \tag{5}$$

so that the direction of $\bar{V}_D$ is along $\hat{y}$ $\left| \frac{\bar{\nabla} n}{n} \right|$ and $\left| \frac{\bar{\nabla} T_e}{T_e} \right|$

are the inverse density and temperature gradient scale lengths, respectively, and we use gaussian cgs units with e defined as the absolute value of electron charge, K the Boltzmann constant and T_e the electron temperature. If in the geometry we consider, electrons are allowed to stream along $\bar{B}$ ($k_z \neq 0$) in an electrostatic approximation, the Boltzmann relation applies to each field line and is,

$$\frac{\delta n}{n} = \frac{e\delta\phi}{KT_e}, \tag{6}$$

where δn is the perturbation in denstiy and $\delta\phi$ is the induced perturbation potential. Associated with the electrostatic oscillations is an azimuthal fluctuating electric field

$$\delta\bar{E} = ik\delta\phi\hat{y} = ik \frac{KT_e}{e} \frac{(\delta n)}{n} \hat{y} \tag{7}$$

where we have used equation (6) with the assumption $\delta\phi = \phi_o e^{-i(ky-\omega t)}$ (Krall and Trivelpiece, 1973; Kelly, 1982). In cylindrical geometry with ∇n_e along r, pressure forces are radial, drift wave propagation to lowest order is azimuthal and surfaces of constant density have a twisted "fluted" appearance (Chen, 1977). In this description we have implicitly maintained the slab geometry x,y,z introduced in equation (4) and shown in Figure 6, thus ignoring the cylindrical curvature of the chamber to first order. Figure 7 is a schematic enlargement of a section of the flute mode azimuthal propagation (Chen, 1977) appropriate to the model at hand. Note that the azimuthal wave vector $\bar{k} = k_y \hat{y}$ is in the direction of drift wave propagation and there is no radial component in this approximation.

To this point we have sketched a zero-order model of drift waves. A brief physical description of this mode in relation to our measurement technique is perhaps appropriate. The nature of the propagation can be described as both longitudinal and transverse (Chen, 1964); that is, since $\bar{k}$ and $\delta\bar{E}$ above are collinear it is longitudinal and, since fluid velocity, $\delta\bar{V}$ produced by $\delta\bar{E}$, is perpendicular to $\bar{k}$ it is also transverse. Using the ideas inherent in this model, δn and $\delta\phi$ are exactly $\frac{\pi}{2}$ out of phase; fluctuations are strictly oscillatory. However, under more realistic conditions (i.e., considering ion inertia, polarization drift etc.) the potential oscillation is observed to lag the density oscillation in many cases by an angle near $\frac{\pi}{4}$ (Hendel and Chu, 1970). In this case wave growth will occur because, in one description, $\delta\bar{V}$ is outward at the same time that the plasma has already moved outward (Chen, 1974). In the linear collisionless case this can occur because of the interaction between resonant electrons and the wave while for the collisional case it occurs because of electron-ion collisions (Ellis and Motley, 1974). In the linear treatment, the drift wave tends to be stabilized

by ion Landau damping and in the collisional regime by ion-ion collisions and the effect of a finite Larmor radius. Assuming a saturation or stabilization mechanism for the present, the relative potential fluctuations can be estimated from the measured density variations as assumed in Equation (6),

$$\text{(i.e.} \quad = \frac{\delta n}{n} \sim \frac{e\delta\phi}{KTe} \quad \text{(Hendel et al, 1968).}$$

Notice then that for a relative density fluctuation of 30% and a thermal temperature of 5000° (.43 ev), $e_{\delta\phi} \sim 130$ millivolts.

For the experimental arrangement we can consider the implications of azimuthal mode propagation in relation to our measurements. Along with measurements of electron density and temperature in Figures 2A and 2B are exponential fits to each data set. With the exponential dependence to these profiles the temperature and density gradient scale lengths are constant. Therefore the electron diamagnetic drift in Equation (4) has a radial dependence which appears through temperature only ($\bar{B}$ constant throughout the measurement domain). In Figure 2C is a plot of the radial dependence of plasma potential as determined from conventional analysis procedures of the E-probe I-V characteristic. Because of the radial dependence of plasma potential there is associated a radially outward electrostatic electric field,

$$\bar{E}_r = -\bar{\nabla}\phi = -\frac{\partial\phi}{\partial r}\hat{r} = +\left|\frac{\partial\phi}{\partial x}\right|_{\text{slab}}\hat{x} \qquad (8)$$

We therefore must include any significant Doppler shift produced in the laboratory frame which is associated with the $\bar{E} \times \bar{B}$ plasma rotation. The rotation direction inferred from the radial field is counter-clockwise in the cylindrical frame and in the ion diamagnetic drift direction (Hendel and Chu,

1968, Ellis and Motley, 1974). Hence a measurement of phase velocity in the laboratory, $\bar{V}_{obs}$, must be corrected by the Doppler velocity, $\bar{V}_E$, to determine wave velocity in the plasma frame or,

$$\bar{V}_{obs} = \bar{V}_E + \bar{V}_{ph} = (V_{ph} - V_{E_{slab}})\hat{y} \tag{9}$$

With the assumption of azimuthal mode propagation the observed velocity, V_{obs}, is related to the observed spectral frequency by,

$$|\bar{V}_{obs}| = \frac{\omega_{obs}}{k_y} = \frac{\omega_{obs}}{m} r, \qquad k_y = \frac{m}{r} \tag{10}$$

where ω_{obs} is the observed radian frequency and we consider an m = 1 rotational mode. In Figure 8 is plotted the frequency component of maximum power for the density fluctuations as determined from observed spectral measurements. Although there is some variation in the observed laboratory frequency, an approximately constant value of 40 Hz is representative of this data set within the measurement accuracy. Plotted in Figure 9 is drift wave phase velocity, $|\bar{V}_{ph}|$, in the plasma frame based on the Doppler shift as seen in Equation (9) where $\bar{V}_E$ is determined from plasma potential measurements as discussed above. Also shown is $|\bar{V}_D|$, the electron diamagnetic drift velocity, which is determined through Equation (4) and the observed temperature and density profiles of Figures 2A and 2B. From Figure 9 and our assumed m = 1 rotational model we see that $V_{ph} \sim V_D/2$ a result predicted by linear theory for maximum growth of the drift instability (Hendel and Chu, 1968). Based therefore on frequency and plasma potential measurements and our model of azimuthal wave propagation these results are consistent with a drift instability interpretation.

Recalling the model of non-local wave propagation discussed in relation to Figure 7, we now consider the time delay associated with phase front motion across the position of our two sensor system. This delay is shown in Figure 10 as a function of radius. It is clear that under an assumption of coherent non-local wave propagation, the measured time delay is simply the difference in times of wavefront arrival at positions E and I. Under an azimuthal mode assumption, such as above, a surface of constant phase necessarily rotates at a constant frequency ω_{obs}, in order that the mode structure remain intact. (Notice that this requirement is fulfilled through the mode assumption expressed in equation (10)). Stating this somewhat differently, the period of azimuthal rotation is constant and independent of radius,

$$\tau = \frac{S(r_1)}{V_{obs}(r_1)} = \frac{S(r_2)}{V_{obs}(r_2)} \tag{11}$$

where $S(r)$ is the circumference and $V_{obs}(r)$ the observed rotational velocity at radius r. A measured time delay ΔT is then the time required to traverse the distance ΔS in Figure 7. (Note that this delay is due to the curvature of the phase front; for rigidly rotating "spokes" the time delay is zero). Because of the constant rotational period the arc length ΔS may be expressed

$$\Delta S(r) = \frac{(\Delta T(r))}{\tau} S(r) \tag{12}$$

Plotted in Figure 10 are arc lengths, ΔS, based on the velocity $V_{obs}(r)$ inferred from frequency measurement and the time delays, ΔT, observed at the two probe locations as a function of radius, i.e.,

$$\Delta T(r) = \frac{\Delta S(r)}{V_{obs}(r)} \tag{13}$$

Other than the fact that these arc lengths are reasonable under model

assumptions, it is difficult to compare the measurements to theory in a more complete manner. This is simply because the model is crucially dependent upon the curvature of the non-local wavefront which is assumed responsible for the measured time delays and this curvature is unknown. It is worth calling the reader's attention further to the fact that the time delay and therefore the curvature is not constant with radius; somewhat as if there is an increasing viscosity or shear (Perkins and Jassby, 1971) in this view.

Combining our plausibility arguments for a drift wave interpretation we now consider the observed spectral distribution of ELF wave energy that corresponds to the density fluctuations which have been the focus of our investigation. Typical spectral behavior, at different positions relative to the beam core, is shown in the lower panels of Figure 2. The observed spectral indices η in an assumed power law dependence $P \propto f^{-\eta}$ were typically in the range 4.5 ± 0.3...a spectral behavior consistent with drift wave characteristics (Chen, 1965; Gary, 1983).

Finally we note that the strongly magnetized plasma electrons which comprise a two component distribution (Szuszczewicz, 1983) of suprathermals and thermals in the beam core and near the beam boundary, were composed primarily of thermal particles in our spatial measurement domain outside the beam core. In addition, we point out that although our zero-order model above describes conditions appropriate to the universal drift instability ($k_z \neq 0 \ll k_y$), an ion Larmor radius r_{Li} of 1.3 m ($T_i \simeq 1500^{\circ}K$), sharp density gradients ($L \sim 1.4$ m) and the introduction of collisions (ion-ion) suggest that an assumption of magnetized ions, as required for positive growth of the collisionless universal instability, is not rigorously maintained. On the other hand, the lower hybrid drift and ion cyclotron instabilities (Huba, Ossakow, 1981a; Gary and Sanderson, 1978) require, abiabatic ions and

perpendicular propagation ($\bar{k} \cdot \bar{B} = 0$, $k_z = 0$) for maximum growth so that the azimuthal diamagetic drift current is carried by the ions. These considerations will affect the conclusions of the equilibrium model above in that the sign of the drift wave frequency will change along with Doppler shift considerations covered earlier. Since the ion and electron diamagnetic drifts will be in opposite directions, and drift wave propagation is in the drift direction, it is straight-forward to separate these two possibilities experimentally with the addition of a third probe in the azimuthal direction. In the present series this configuration was not in place so that we are unable to unambiguously determine a drift wave propagation direction.

Under this constraint, however, and based upon further characterization of the plasma, there are some conclusions with regard to possible instabilities present. For the particular series considered the neutral (N_2) background density can be taken as 6×10^{10} cm^{-3} ($P \sim 10^{-5}$ Torr). In our temperature measurement regime outside the beam core ($.1ev \lesssim T_e \lesssim .5ev$) electron-ion collisions dominate over electron-neutral collisions with $\nu_{ei} \sim (5\text{-}30)\ \nu_{en}$ (Braginski, 1965; Banks, 1966a). Ion neutral collisions, on the other hand, dominate ion collisions with $\nu_{in} \sim (15\text{-}130)\ \nu_{ii}$. These collision estimates then provide some basis for comparison to the collisional lower hybrid drift instability. With strongly magnetized electrons ($r_{Le} \sim 1$ cm at $T_e = .5ev$) and the possibility of ion resonance with the wave (e.g. ion-ion collisions can effectively demagnetize ions so they are able to participate in resonance with a perpendicularly propagating wave), wave growth can occur. For this case one finds that electron collisions ($\nu_e \sim (.2\text{-}1)$kHz) provide viscosity to absorb wave energy and effectively place a threshold condition on wave growth (Huba, Ossakow; 1981b). The condition is,

$$\left(\frac{kV_i}{\nu_e}\right)^{1/2} > \frac{L}{r_{Li}} \sim 1$$

or

$$kV_i > \nu_e$$

where V_i is the ion thermal velocity, ν_e is the total electron collision frequency and L is the density gradient scale length. Since the model we employ is based on coherent non-local wave propagation ($L < k^{-1}$) and we assume that azimuthal wavelengths are comparable (Chen, 1967), we have,

$$kV_i \backsim 70 \text{ sec}^{-1} \qquad (k \backsim .001 \text{ cm}^{-1},\ T_i \approx 1500^{\circ}K)$$

Therefore within our temperature range this threshold is not reached. In addition, the fact that this instability is primarily applicable in the short wavelength regime ($r_{Li} >> k^{-1}$) would tend to strengthen an argument against it in the present case where $kr_{Li} \backsim 0.1$. More detailed arguments must await a numerical solution of the dispersion relation under the conditions existing in the chamber during the BPD measurement.

Finally, we point out that the instability destabilization (or wave growth) which occurs in transition to BPD can derive its energy from a number of free energy reservoirs available (i.e., temperature and density in homogeneity (presure gradient), radial velocity shear). For our experimental conditions ($kr_{Le} << 1$, $kr_{Li} \lesssim 1$, $\nu_e >> \omega$) the pressure gradient ($\bar{\nabla} n_e$, $\bar{\nabla} T_e$) is perhaps the most likely candidate to contribute to destabilization. For example, in the case of the temperature gradient the growth rate for long wavelength collisional drift waves under the conditions above has been shown to vary with temperature gradient in Q-machines (Yamada and Hendel, 1978).

V. CONCLUSIONS

We have obtained spectra of density oscillations in a cylindrical magnetized plasma with temperature and density gradients during the BPD instability which occurred at an electron beam voltage of 1.6 kev and a beam current of 40 ma. We have measured the electron density, temperature, plasma potential and cross-correlation time delays associated with the oscillations at separate radial positions using the P^3 system. A zero order equilibrium drift wave model along with an $\bar{E} \times \bar{B}$ drift has been compared to the results of measurement. Based on an $m = 1$ mode assumption, drift wave phase velocity is estimated at near one half the electron diamagnetic drift speed if Doppler corrected velocities are used. The model comparison is offered as a plausible explanation of the observations based on comparisons to theory.

VI. ACKNOWLEDGMENT

We would like to thank J. Huba, P. Rodriguez and P. Chaturvedi for helpful discussions during this work. Support for this project was provided by the Office of Naval Research. Experimental support at the Johnson Space Center was provided under NASA/NOAA contract #NA79RAA04487.

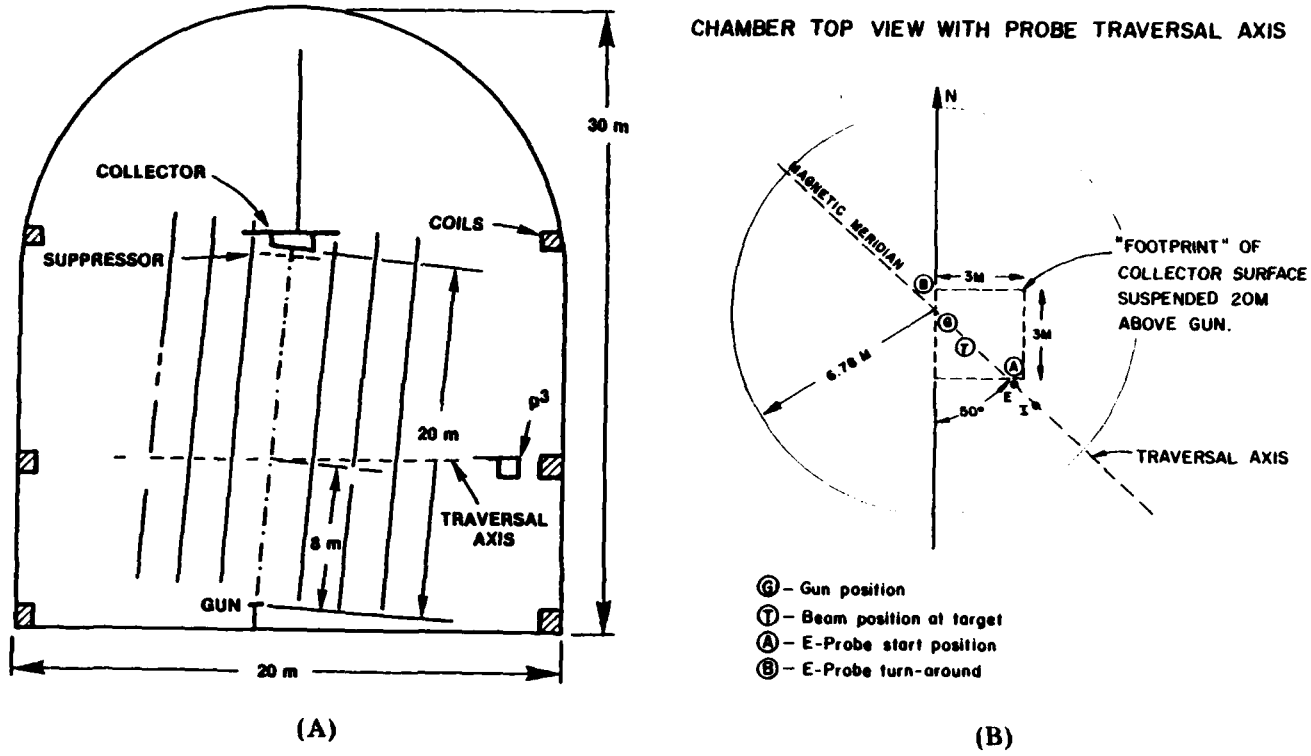

Fig. 1 — (A) Side view of the experimental configuration in the large chamber at the Johnson Space Center and (B) top view of probe traversal axis showing location with respect to the electron beam gun and target.

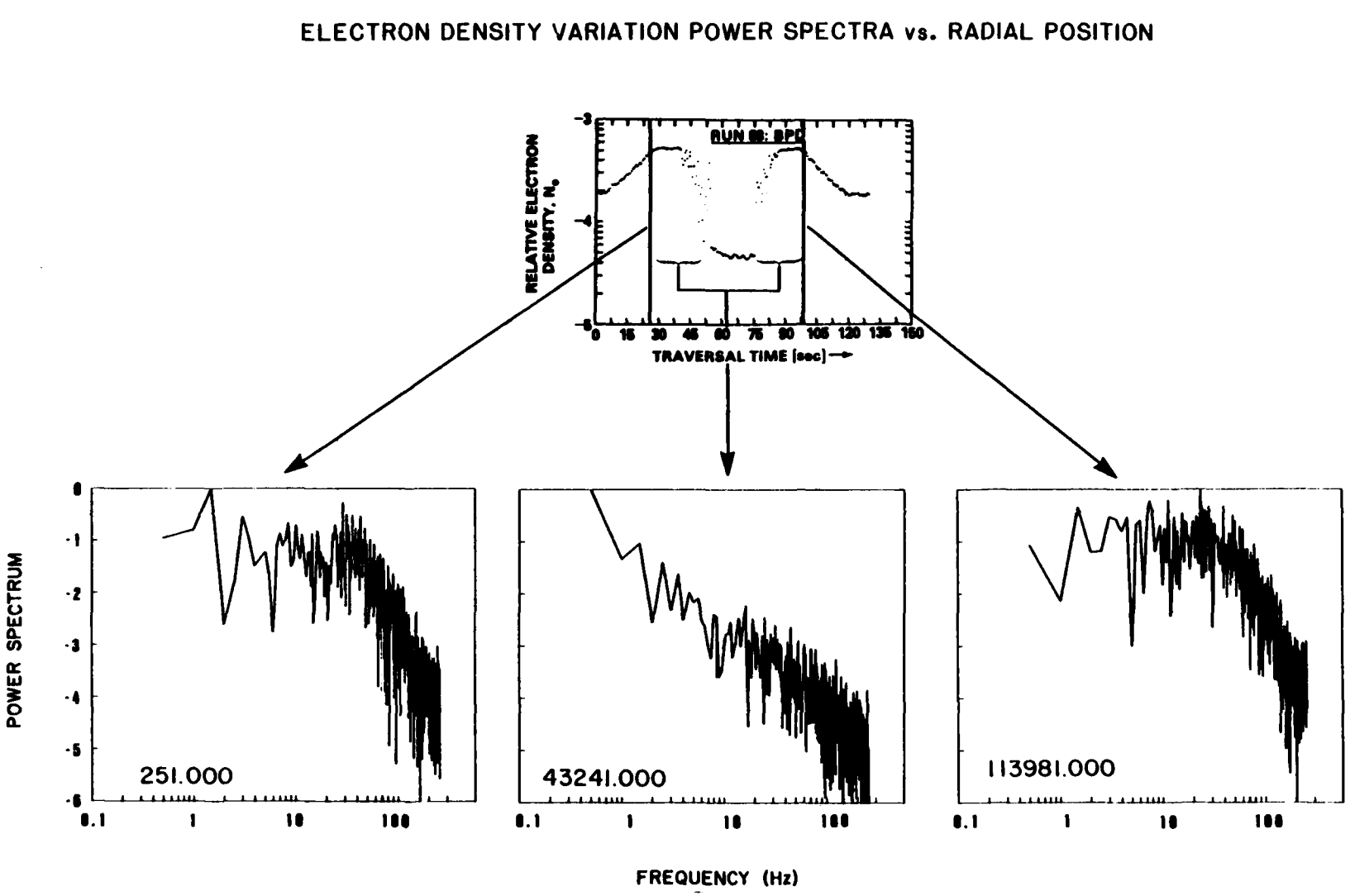

Fig. 2 — Power spectral and radial electron density profile during an in-out traversal. Relative electron density is plotted versus traversal time. The traversal rate was approximately .07 m/sec. The distance of the E-probe (I-probe) from beam center at t=o is approximately 2.4 (3.4) meters.

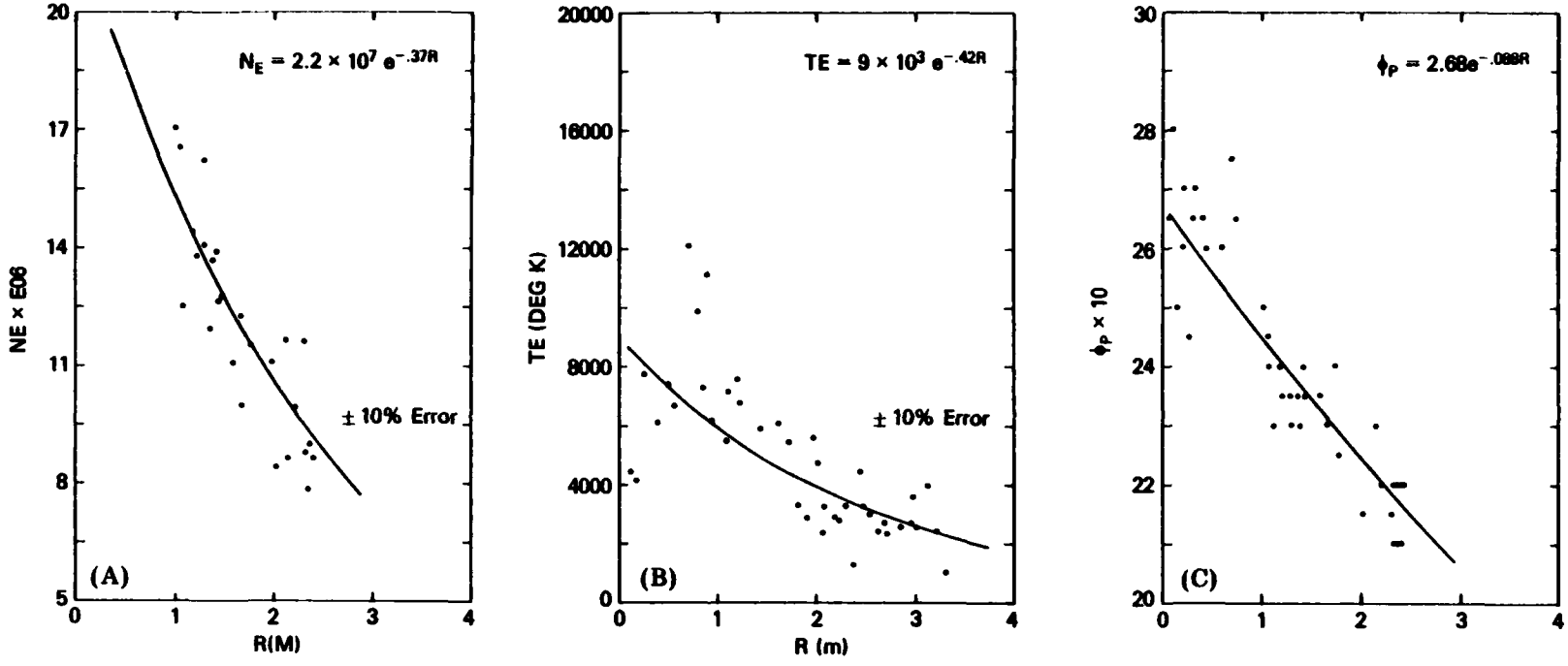

Fig. 2(A) — Electron density and exponential fit vs radius from beam center; (B) electron temperature and exponential fit vs radius from beam center; and (C) plasma potential and experimental fit vs radius from beam center.

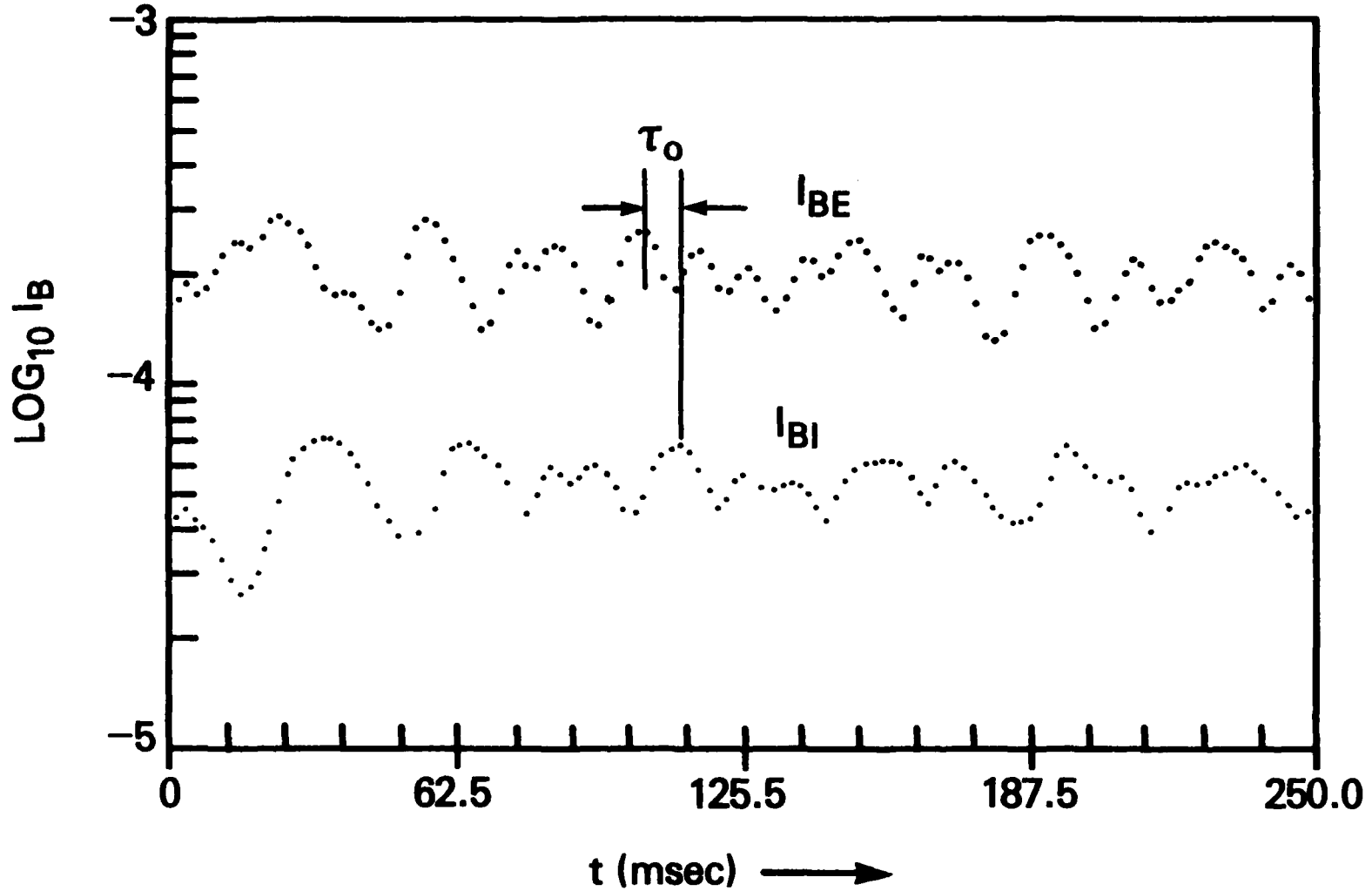

Fig. 3 — Electron (I_{BE}) and Ion (I_{BI}) saturation currents collected by the E and I probe, respectively. Ion currents have been multiplied by -1 for comparison τ_o is the phase difference between I_{BE}, I_{BI}.

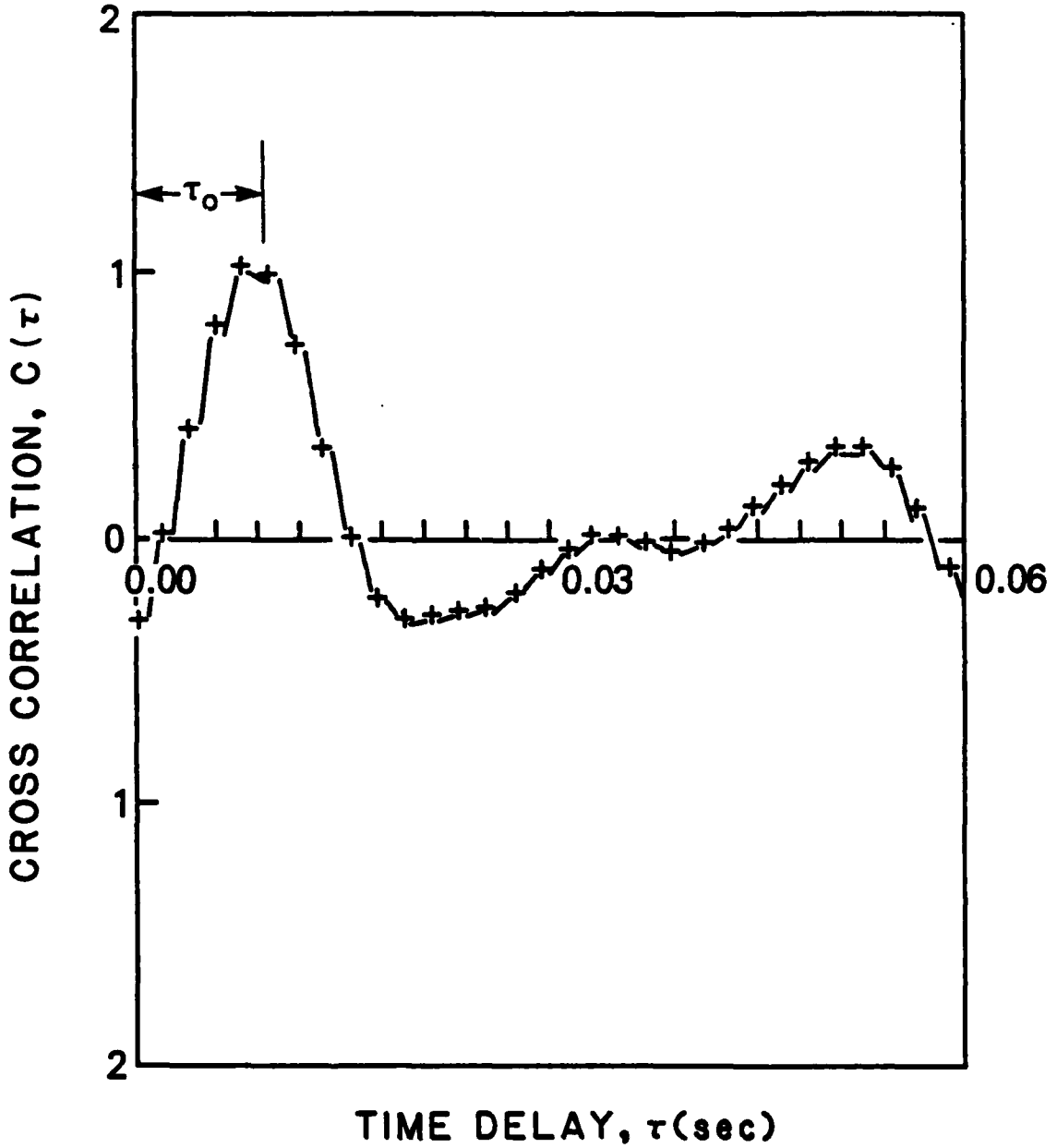

Fig. 4 — Cross-correlation integral, $C(\tau)$, of normalized electron and ion saturation current variations using the I_{BE}, I_{BI} segment shown in Figure 2.

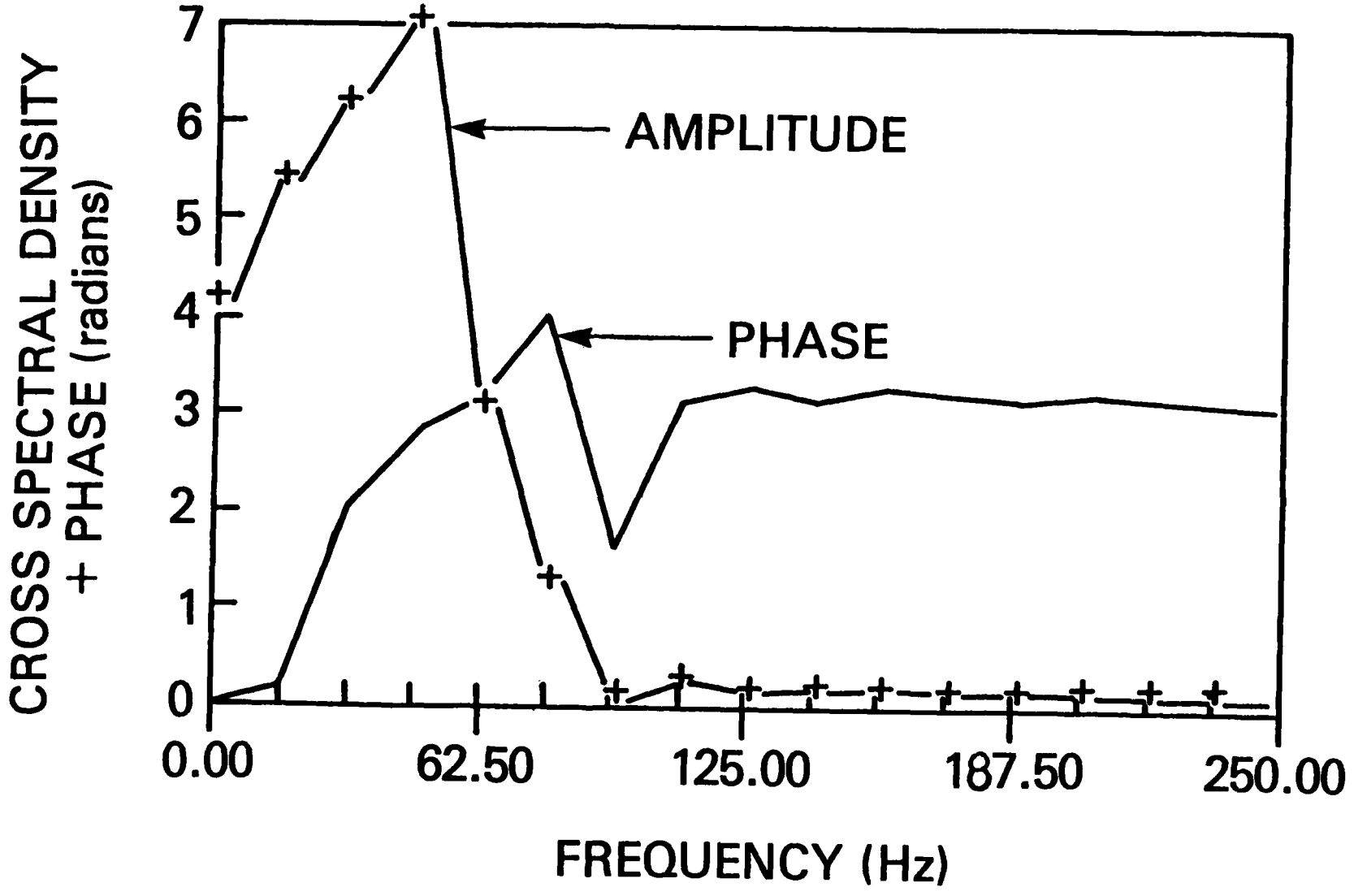

Fig. 5 — Cross-spectral density amplitude and phase obtained from the Fourier transform of $C(\tau)$.

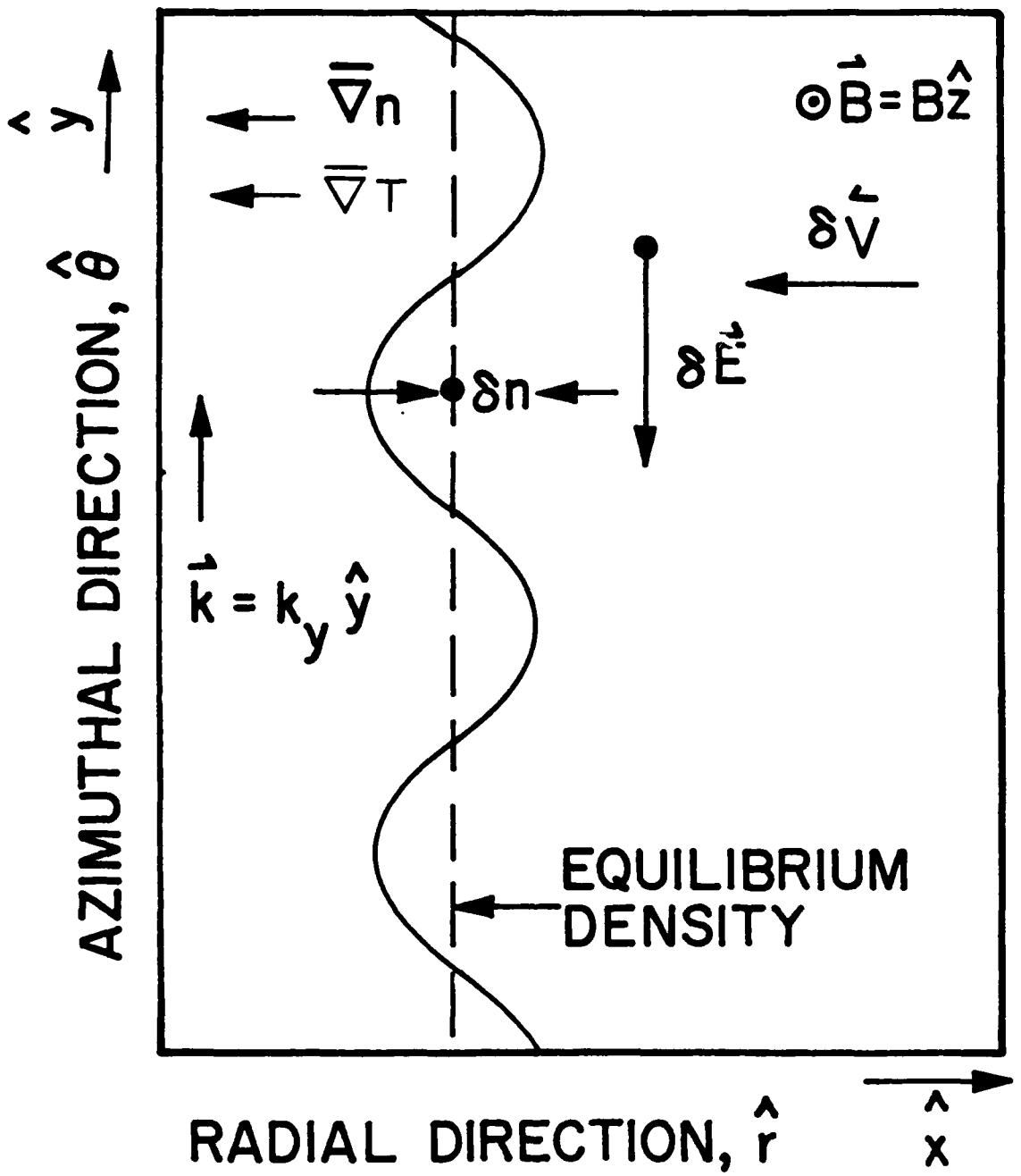

Fig. 6 — Enlargement of a section of flute mode oscillation showing the coordinate system employed in the mode (F.F. Chen, 1977).

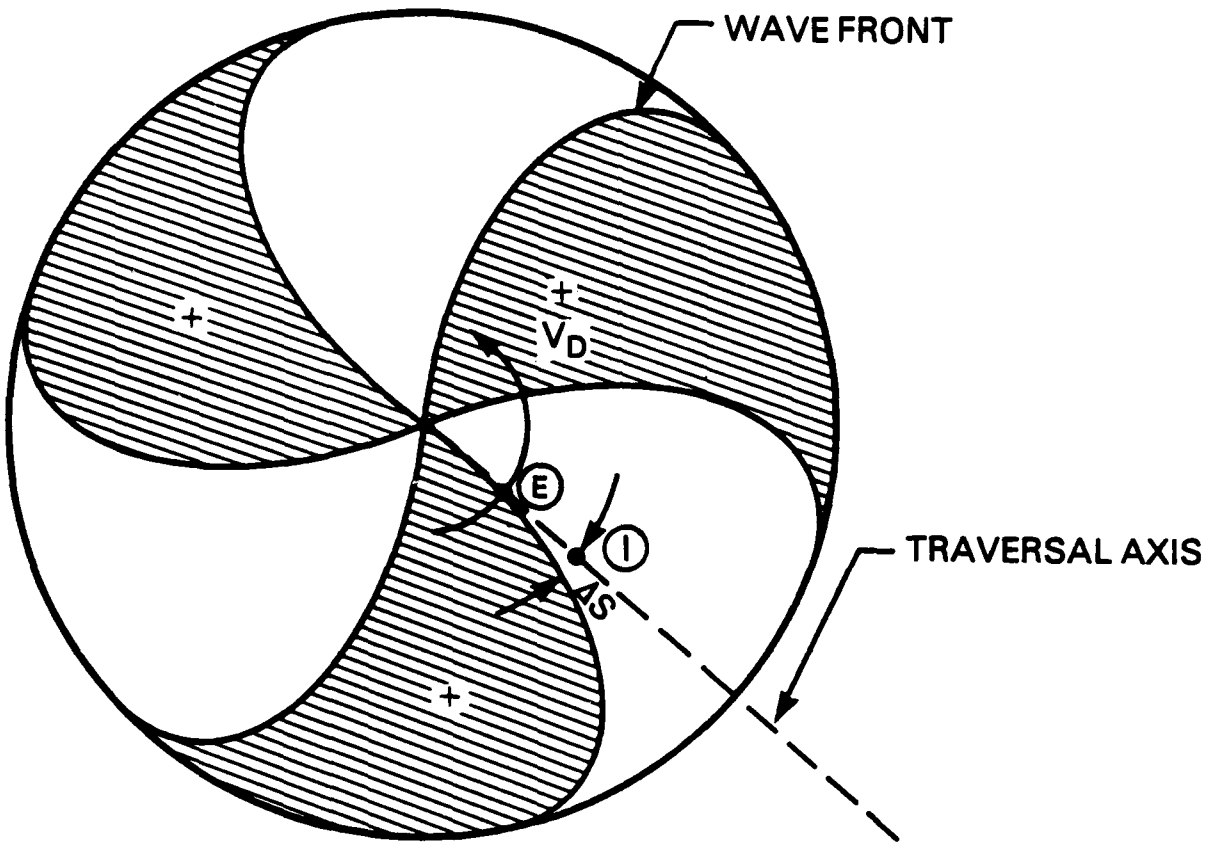

(E) E-PROBE REPRESENTATIVE POSITION

(I) I-PROBE REPRESENTATIVE POSITION

Fig. 7 — Chamber top view of an m=3 azimuthal mode with probe traversal axis

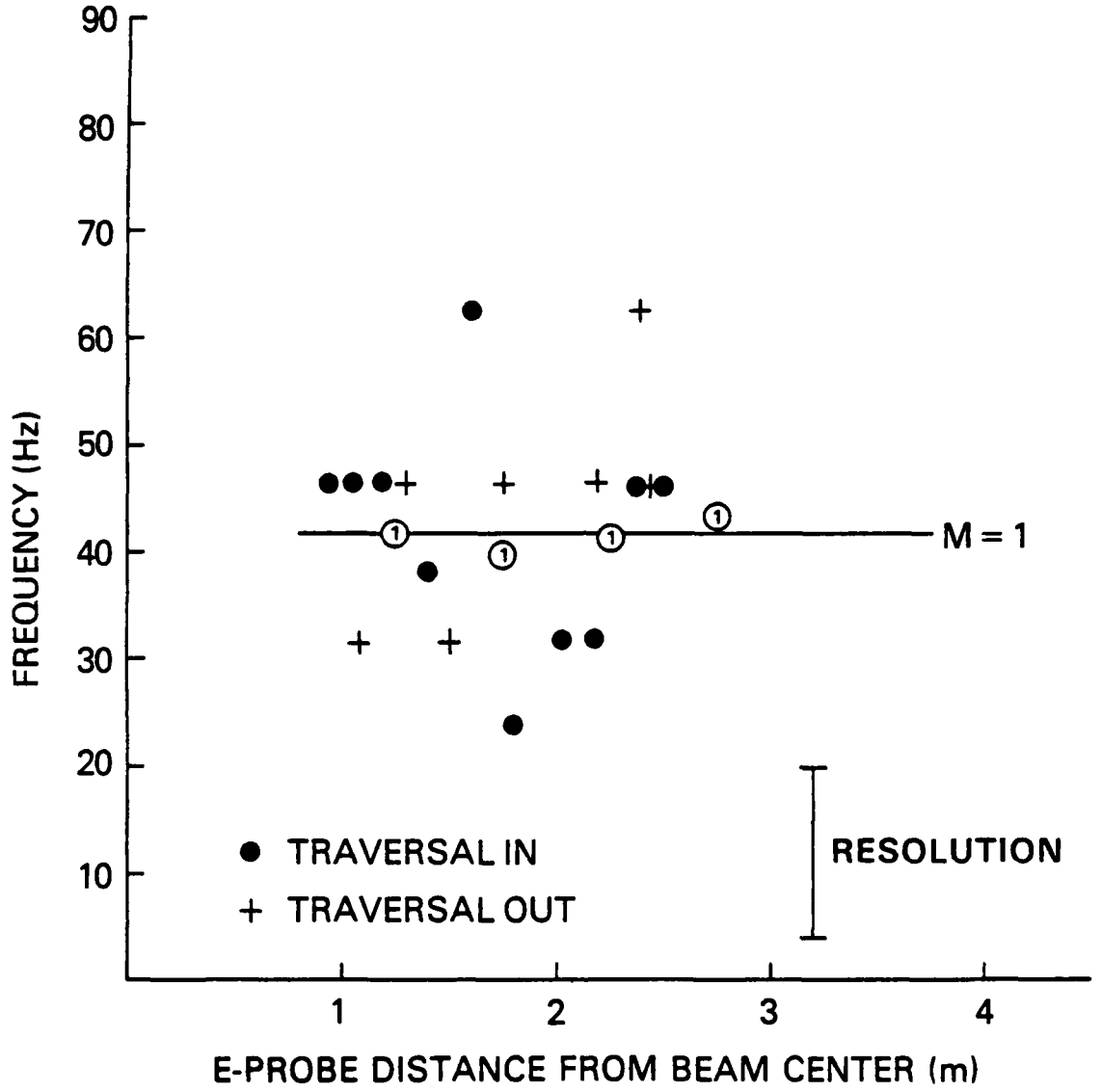

Fig. 8 — Major frequency component of spectra as a function of radial position with m=1 calculated results

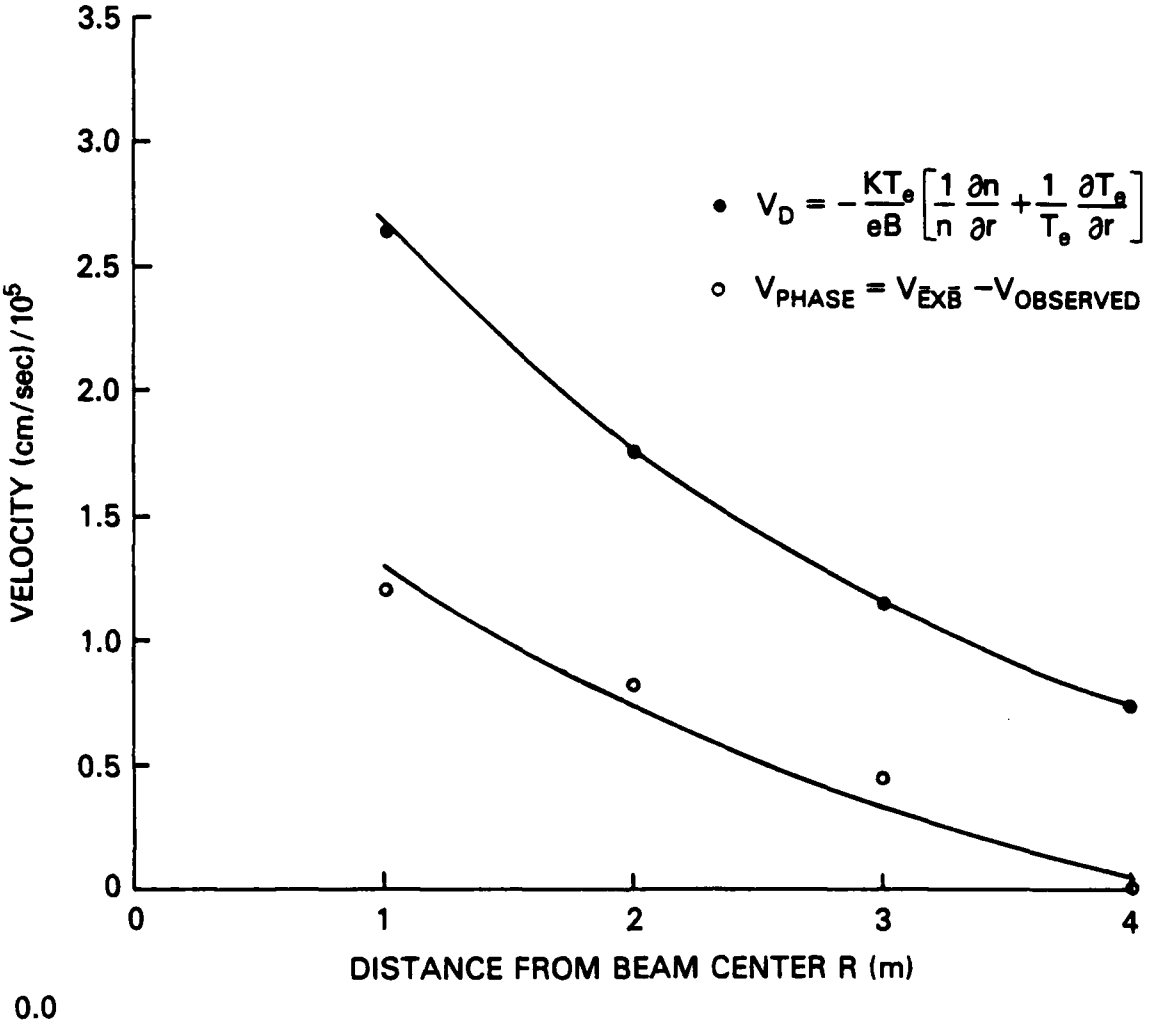

Fig. 9 — Measured electron diamagnetic drift V_D and measured V_{ph} (corrected for Doppler) vs radial position

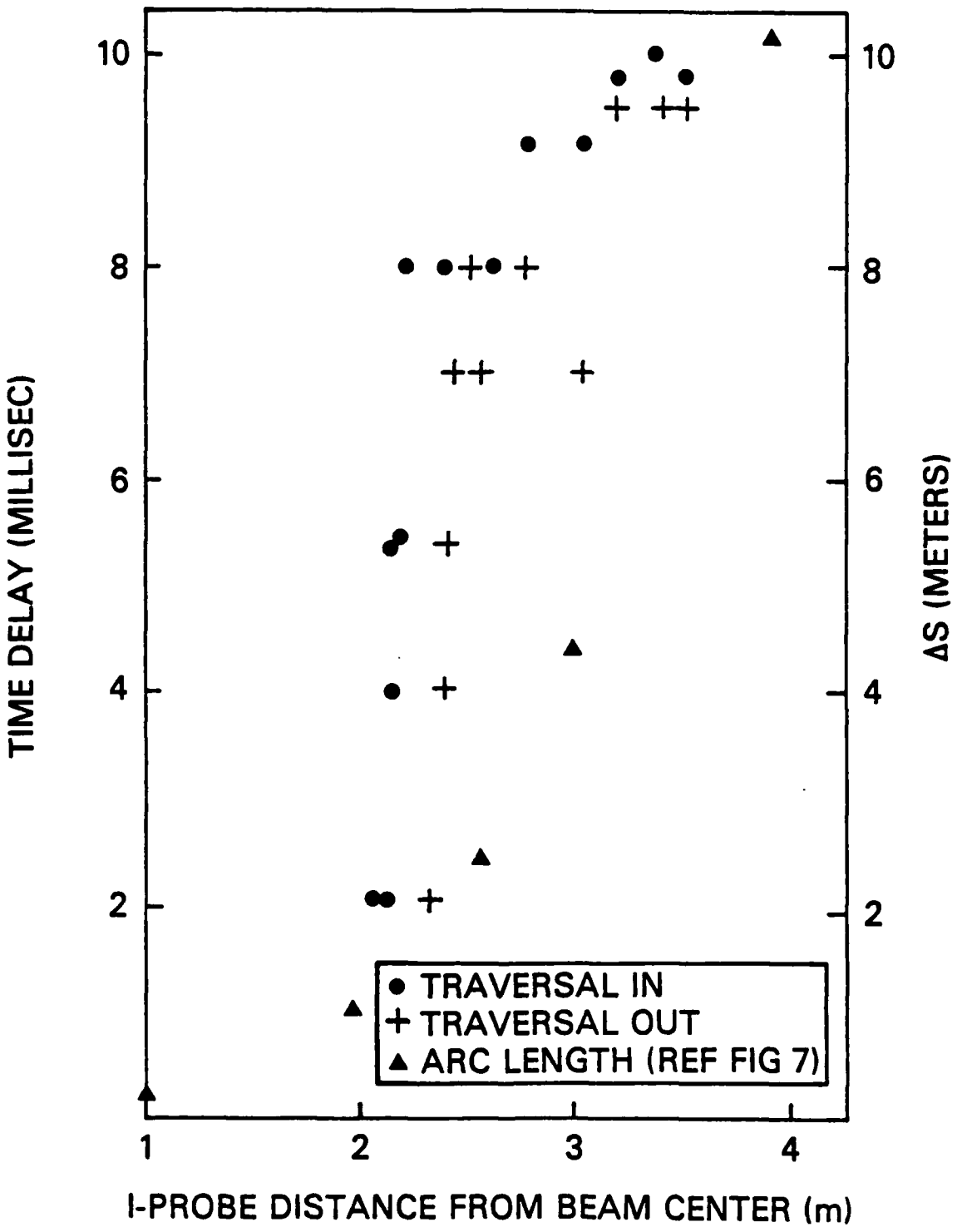

Fig. 10 — Measured time delay between the two probe positons from cross correlation results

REFERENCES

Anderson, H.R., R.J. Jost, and J. Gordenk, (1981) Electron Energy Distribution Produced by Beam-Plasma-Discharge, NATO Advanced Research Institute, Geilo, Norway, in Artificial Particle Beams Utilized in Space Plasma Physics, Plenum Publishing Co., New York.

Bendat, J.S., and A.G. Piersol, (1971), Random Data: Analysis and Measurement Procedures, Wiley Interscience.

Bernstein, W., H. Leinbach, P. Kellogg, S. Monson, T. Hallinan, O.K. (1978), Electron Beam Injection Experiments: The Beam-Plasma Discharge at Low Pressures and Magnetic Field Strengths, Geophys. Res. Lett., 5, 127.

Bernstein, W., H. Leinbach, P.J. Kellogg, S.J. Monson, and T. Hallinan, (1979), Further Laboratory Measurements of the Beam-Plasma Discharge, J. Geophys. Res., 84, 7271.

Cambou, F., V.S. Dokoukine, V.N. Ivchenko, G.G. Managadze, V.V. Migulin, O.K. Nazarenko, A.T. Nesmyanovich, A.K. Pyatsi, R.Z. Sagdeev, and I.A. Zhulin, (1975), The Zarnitza Rocket Experiment on Electron Injection, Space Research, XV, 491.

Cambou, F., J. Lavergnat, V.V. Migulin, A.I. Morozov, B.E. Paton, R. Pellat, A. Kh. Pyatsi, H. Reme, R.Z. Sagdeev, W.R. Sheldon, and I.A. Zhulin, (1978), ARAKS-Controlled or Puzzling Experiment? Nature, 271, 723.

Chen, F.F., (1964), Normal Modes for Electrostatic Ion Waves in an Inhomogeneous Plasma, Phys. Fluid, 7, 949.

Chen, F.F., (1965), Spectrum of Low-β Plasma Turbulence, Phys. Rev. Lett., 15, 381.

Chen, F.F., (1965), "Universal" Overstability of a Resistive, Inhomogeneous Plasma, Phys. Fluids, 8, 1323.

Chen, F.F., (1966), Microinstability and Shear Stabilization of a Low-β, Rotating, Resistive Plasma, Phys. Fluids, 9, 965.

Chen, F.F., (1967), Nonlocal Drift Modes in Cylindrical Geometry, Phys. Fluids, 10, 1647.

Chen, F.F., (1977), Introduction to Plasma Physics, Plenum Press. (Page 195 (Figure 6-17) includes a relevant discussion to model assumptions).

Ellis, R.F. and R.W. Motley, (1974), Current-Driven Collisional Drift Instability, Phys. Fluids, 17, 582.

Gary, S.P. and J.J. Sanderson, (1978), Density Gradient Drift Instabilities: Oblique Propagation at Zero Beta, Phys. Fluids, 21 (7), 1181.

Gary, S.P., (1980), Wave-Particle Transport from Electrostatic Instabilities, Phys. Fluids, 23, 1193.

Gary, S.P., Bernhardt, P.A. and Cole, T.E. (1983), Density Drift Instabilities and Weak Collisions, J. Geophys. Res., 88, 2103.

Getty, W.D., and L.D. Smullin, (1963), Beam-Plasma Discharge: Buildup of Oscillations, J. Appl. Phys., 34, 3421.

Hendel, H.W., T.K. Chu and P.A. Politzer, (1968), Collisional Drift Waves-Identification, Stabilization, and Enhanced Plasma Transport, Phys. Fluids, 11, 2426.

Hendel, H.W. and T.K. Chu, (1970), Collisional Drift Instabilities, Methods of Experimental Physics, 9(A), 345. [Plasma physics, H.R. Griem, ed. Pt. 1]

Hooper, E.B., (1970), Characteristics of a Reflex Arc: Low Magnetic Field Mode, Plasma Physics, 12, 855.

Hooper, E.B., G.A. Hallock and J.H. Foote, (1983), Low-Frequency Oscillations in the Central Cell of the TMX Tandem Mirror Experiment, Phys. Fluids, 26, 314.

Huba, J.D. and S.L. Ossakow, (1979), On the Generation of 3-m Irregularities During Equatorial Spread F by Low-Frequency Drift Waves, J. Geophys. Res., 84, 6697.

Huba, J.D. and S.L. Ossakow, (1981), On 11-cm Irregularities During Equatorial Spread F, J. Geophys. Res., 86, 829.

Huba, J.D. and S.L. Ossakow, (1981), Physical Mechanism of the Lower-Hybrid-Drift Instability in a Collisional Plasma, J. Atmos. and Terr. Phys., 43, 775.

Kadomtsev, B.B., Plasma Turbulence, Academic Press, New York, 1965.

Kelley, M.C., (1982), Nonlinear Saturation Spectra of Electric Fields and Density Fluctuations in Drift Wave Turbulence, Phys. of Fluids, 25(6) 1002.

Krall, N.A., and A.W. Trivelpiece, (1973), Principles of Plasma Physics, McGraw-Hill.

Ossakow, S.L., (1981), Spread-F Theories - A review, J. Atmos. Terr. Phys., 43, 437.

Papadopoulos, K., (1982, in press) Theory of Beam-Plasma-Discharge, NATO Advanced Research Institute, Geilo, Norway (1981), in Artificial Particle Beams Utilized in Space Plasma Physics, Plenum Publishing Co., New York.

Perkins, F.W. and D. L. Jassby, (1971), Velocity Shear and Low-Frequency Plasma Instabilities, Phys. Fluids, 14, 102.

Rudakov, L.I., R.Z. Sagdeev, (1961), On the Instability of a Nonuniform Rarefied Plasma in a Strong Magnetic Field, Sov. Phys., Dokl 6, 415.

Singh, M. and E.P. Szuszczewicz, (1984), Composite Equatorial Spread F wave Number Spectra from Medium to Short Wavelengths, J. Geophys. Res., 89, 2313.

Smullin, L.D., (1981), A Reivew of the Beam-Plasma-Discharge, in Relation Between Laboratory and Space Plasmas, Hiroshi Kikuchi, editor, D. Reidel Publishing Co., (Dordrecht/Boston/London), pp. 4566.

Szuszczewicz, E.P., D.N. Walker, and H. Leinbach, (1979), Plasma Diffusion in a Space Simulation Beam-Plasma-Discharge, Geophys. Res. Lett., 6, 201.

Szuszczewicz, E.P., K. Papadopoulos, W. Bernstein, C.S. Lin, and D.N. Walker, (1982a), Threshold Criteria for a Space-Simulation Beam-Plasma-Discharge, J. Geophys. Res., 87, 1565.

Szuszczewicz, E.P., (1982b), The S3-4 Ionospheric Irregularities Experiment; Probe Detection of Multi-Ion Component Plasmas and Associated Effects on Instability Processes, Astrophys. and Space Sci., 86, 235.

Szuszczewicz, E.P., (1983), Direct Measurements of Plasma Characteristics in Space Simulation Beam-Plasma Interactions, AIAA J., (in press).

Yamada, M. and H.W. Hendel, Current-Driven Instabilities and Resultant Anomalous Effects in Isothermal, Inhomogeneous Plasmas, Phys. Fluids, 21, 1555.

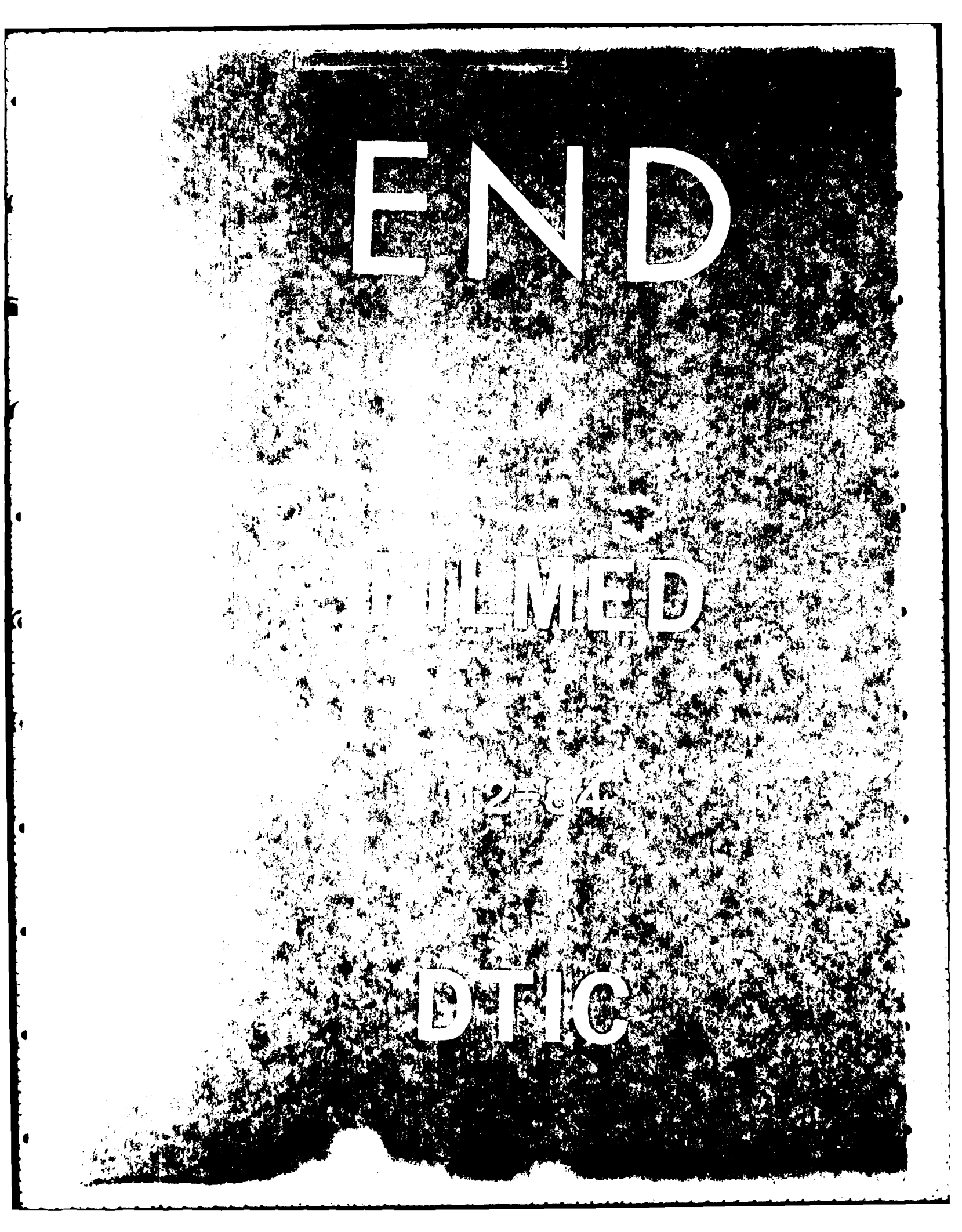
END
LIMED
DTIC